Supporting Information

Goldberg *et al.* 10.1073/pnas.0807942105

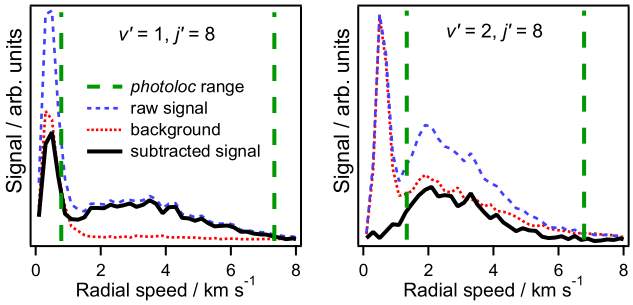

Fig. S1. Representative radial speed distributions used to obtain the differential cross-sections $I(\theta)\sin\theta$ for $D_2(v' = 1,2, j' = 8)$ at $E_{coll} = 1.7$ eV. The corrected signal (black line) is calculated by subtracting the background (red dotted line) from the raw signal (blue dashed line). The region between the heavy dashed lines corresponds to the range of allowed speeds for inelastic scattering with fast-channel H atoms (Table S1). Nonresonantly ionized $D_2(v = 0)$ contaminates the signal at slow speeds. For $v' = 2$, resonant background caused by HBr photolysis and subsequent inelastic scattering within the duration of the probe laser pulse is subtracted; for $v' = 1$ there is an additional $D_2(v = 1)$ resonant background at slow speeds that cannot be subtracted.

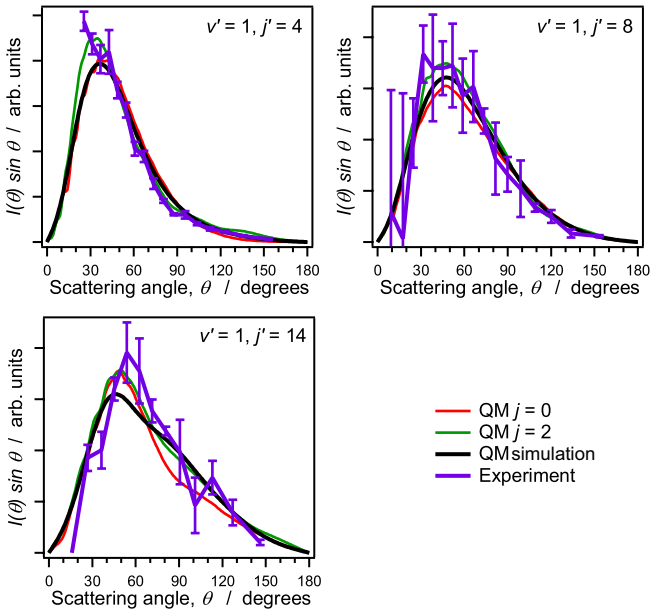

Fig. S2. Comparison of measured differential cross-sections for $D_2(v' = 1, j' = 4,8,14)$ formed at $E_{coll} = 1.76$, 1.73, and 1.65 eV, respectively (purple lines), with fully converged quantum mechanical calculations (black lines). Calculated contributions from $D_2(v = 0, j = 0)$ and $D_2(v = 0, j = 2)$ reactants are shown separately (red and green lines, respectively). The black lines are averages of the contributions from $D_2(v = 0, j = 0)$ and $D_2(v = 0, j = 2)$ weighted to match the fractions of these components present in the molecular beam and blurred to match the velocity resolution of the experiment. Error bars on the purple lines represent 1 standard deviation.

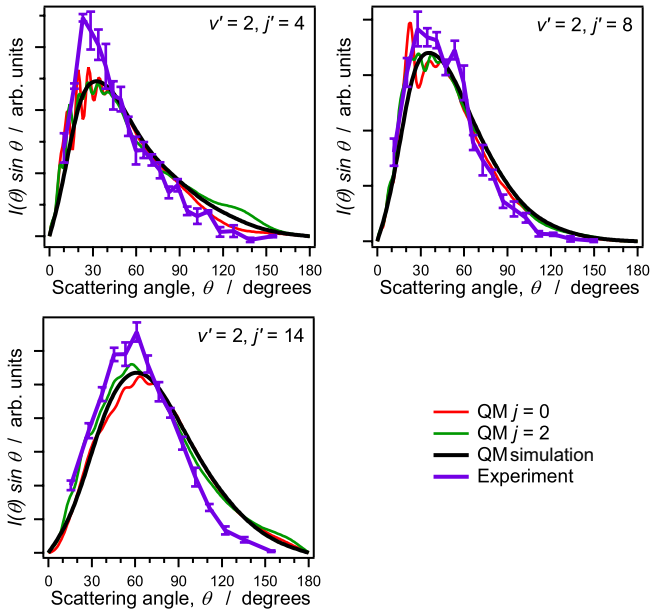

Fig. S3. Comparison of measured differential cross-sections for $D_2(v' = 2, j' = 4,8,14)$ formed at $E_{coll} = 1.72$ eV (purple lines) with fully converged quantum mechanical calculations (black lines). Calculated contributions from $D_2(v = 0, j = 0)$ and $D_2(v = 0, j = 2)$ reactants are shown separately (red and green lines, respectively). The black lines are averages of the contributions from $D_2(v = 0, j = 0)$ and $D_2(v = 0, j = 2)$ weighted to match the fractions of these components present in the molecular beam and blurred to match the velocity resolution of the experiment. Error bars on the purple lines represent 1 standard deviation.

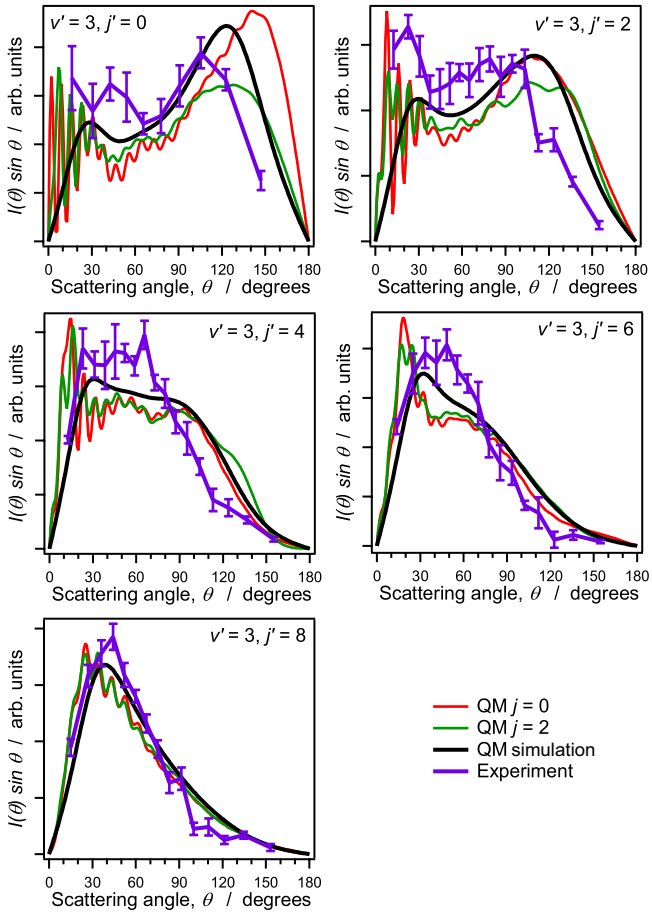

Fig. S4. Comparison of measured differential cross-sections for $D_2(v' = 3, j' = 0,2,4,6,8)$ formed at $E_{coll} = 1.72$ eV (purple lines) with fully converged quantum mechanical calculations (black lines). Calculated contributions from $D_2(v = 0, j = 0)$ and $D_2(v = 0, j = 2)$ reactants are shown separately (red and green lines, respectively). The black lines are averages of the contributions from $D_2(v = 0, j = 0)$ and $D_2(v = 0, j = 2)$ weighted to match the fractions of these components present in the molecular beam and blurred to match the velocity resolution of the experiment. Error bars on the purple lines represent 1 standard deviation. For reasons that are presently unknown, the agreement is worse for the lowest values of j'. A qualitatively similar discrepancy was seen in ref. 1 for the reactive $HD(v' = 3, j' = 0)$ channel, which is related to the present work because of extensive transition-state recrossing. That discrepancy was believed to arise from the presence of rotationally excited D_2 reactants. In the present work, the inclusion of $D_2(v = 0, j = 2)$ reactants improves the agreement, but slight differences remain.

1. Goldberg NT, Zhang J, Miller DJ, Zare RN (2008) Corroboration of theory for $H+D_2 \rightarrow D+HD(v'=3,j'=0)$ reactive scattering dynamics. *J Phys Chem A* 112:9266–9268.

Table S1. Summary of experimental parameters for H + D_2(v = 0, j = 0,2) → H + D_2(v', j') differential cross-sections

			Laboratory speed range (km s^{-1})		
v'	j'	Nominal collision energy,* eV	Fast	Slow	No. of angles in DCS
1	4	1.76	0.53–7.68	0.60–6.73	17
1	8	1.73	0.79–7.35	0.91–6.34	18
1	14	1.65	1.57–6.38	1.99–5.05	13
2	4	1.72	1.05–7.08	1.24–5.99	22
2	8	1.72	1.34–6.79	1.61–5.62	18
2	14	1.72	2.17–5.96	3.20–4.04	15
3	0	1.72	1.52–6.61	1.87–5.37	10
3	2	1.58	1.67–6.12	2.19–4.66	15
3	2	1.72	1.56–6.57	1.92–5.31	17
3	4	1.58	1.77–6.02	2.39–4.47	15
3	4	1.72	1.65–6.48	2.06–5.17	17
3	4	1.94	1.49–7.14	1.77–6.03	20
3	6	1.72	1.79–6.33	2.30–4.93	16
3	8	1.72	2.01–6.12	2.72–4.52	15
3	8	1.94	1.80–6.84	2.19–5.61	18
4	0	1.82	2.09–6.27	2.78–4.71	13
4	2	1.82	2.14–6.22	2.89–4.61	13
4	4	1.82	2.24–6.11	3.19–4.31	12
4	6	1.82	2.43–5.94	Not allowed	11

*Photolysis of HBr proceeds by 2 different channels, each of which deposits a different amount of translational energy in the H atom reactant. The collision energy of the minor (slow) channel is 0.36 eV smaller than that of the major (fast) channel.